Electrochemical Studies of BiTeSe Films Deposition from Ionic Liquids Based on Choline Chloride with Ethylene Glycol, Malonic Acid or Oxalic Acid

CAMELIA AGAPESCU[1], ANCA COJOCARU[1]* , FLORENTINA GOLGOVICI[2], ADRIAN CRISTIAN MANEA[1], ADINA COTARTA[1]

[1]University Politehnica Bucharest, Department of Inorganic Chemistry, Physical Chemistry and Electrochemistry, 132 Calea Grivitei, 010737, Bucharest, Romania

[2] University Politehnica Bucharest,Department of General Chemistry, 1-7 Polizu Str., 011061, Bucharest, Romania

The processes during the electrodeposition/dissolution of BiTeSe films on Pt and Cu electrodes were investigated by cyclic voltammetry and electrochemical impedance spectroscopy experiments. The electrolytes used were ionic liquids based on choline chloride mixed with ethylene glycol, malonic acid or oxalic acid, and the working temperature was 60 ^{0}C. Scanning the potential negatively, as a three-step mechanism, elemental selenium is first deposited at less negative potentials, followed by a direct formation of BiSeTe film and a Bi-rich ternary film. In the last step, the massive bismuth deposition proceeds together with hydrogen evolution and probably with reduction of choline cation. Deposition of BiTeSe films has been carried out in mixtures of choline chloride with malonic acid or oxalic acid on Cu plates in galvanostatic or potentiostatic conditions at 60 ^{0}C. Their characterization was performed using corrosion tests (Tafel plots, electrochemical impedance spectra).

Keywords: electrodeposition, bismuth telluroselenide, ionic liquid, choline chloride, corrosion

Compounds of tellurium and selenium as binary and ternary semiconductors are involved in a wide range of applications [1-3]: solar cells, photoelectrochemical and thermoelectrical devices, micromechanical systems, optical filters, optical recording materials, superionic materials, as well as sensor and laser materials. As an example, bismuth telluroselenides having $Bi_2Te_{2.7}Se_{0.3}$ composition are recognized as thermoelectric materials with the best Seebeck coefficient at room temperature. Obviously, all these applications play an important role in a global sustainable development.

The electrochemical preparation of $Bi_2(Te,Se)_3$ semiconductor compounds [2-11] has attracted considerable interest because of the advantages of electrolysis procedure than other physical, chemical or metallurgical procedures. Historically, the electroplating of BiTeSe films, as well as preparation of ternary nanowires or nanotubes, has been carried out since 2003 [4,5] using aqueous baths. The cathodic process implies the presence in the bath of all three elements (introduced as dissolved precursors), but the weak solubility of bismuth and chalcogenide compounds (salts, oxides) imposes generally an acidic electrolyte. In most papers concerning BiTeSe electrodeposition nitric acid aqueous solution was used, even if sometimes other acid electrolytes (HCl, $HClO_4$ or H_2SO_4 solutions) were chosen. The recommended baths (1M HNO_3 solutions) contain generally 1-10mM concentrations of Bi^{3+}, Te^{4+} (as $HTeO_2^+$) and Se^{4+} (as $HSeO_2^+$) ionic species. The selection of deposition voltage and metallic support nature were performed usually by cyclic voltammetry tests.

In the recent years, because room temperature ionic liquids were increasingly applied for electrochemical purposes, the electroplating of tellurium and selenium compounds films has been demonstrated, for instance using 1-butyl-1-methylpyrrolidinium bis (trifluoromethyl-sulfonyl) amide or 1-ethyl-3-methylimidazolium tetra-fluoroborate / chloride) as more environmentally friendly media alternative [12-14]. The advantages of these novel baths include: extended electrochemical window; extremely low vapour pressures; significantly reduced hydrogen evolution as compared with the acidic aqueous baths conventionally employed; easy to achieve deposition of a desired composition of semiconductor deposit; lower electrical energy consumption comparing with aqueous solutions. The greater thermal stability and higher conductivity of the ionic liquid is useful to obtain crystalline semiconductor films through direct electrodeposition at higher temperatures without subsequent annealing.

We recently have shown the possibility of electrodeposition of Bi, Te and Se as elements or binary compounds using ionic liquids consisted in eutectic mixtures of choline chloride (2-hydroxy-ethyl-trimethyl ammonium chloride) with urea [15,16], malonic acid [17,18] or ethylene glycol [19]. In this paper, we present the cyclic voltammetry and electrochemical impedance spectroscopy results regarding the electrodeposition at 60^{0}C of BiTeSe films from three choline chloride (ChCl) based ionic liquids, i.e. mixtures of ChCl with ethylene glycol (EG), malonic acid (MA) or oxalic acid (OxA). These ionic liquids used in the present work were first developed by Abbott et al. [20] and consist of deep eutectic mixtures due to hydrogen bonding interactions between EG, MA or OxA and chloride ions from ChCl.

The characterization of films grown on Cu substrate by long time electrolysis was made by corrosion tests. The stability of BiTeSe films against aggressive media, including marine environment, has relevance for thermoelectric and photoelectrochemical applications, improving the efficiency of thermoelectric devices or solar cells. In this respect, we mention that despite of some preliminary studies [18,21] the corrosion resistance of such semiconductor films has not been extensively studied.

* *email: a_cojocaru@chim.upb.ro; Tel. 021/4023962*

Experimental part

The investigated ionic liquids as background electrolytes were prepared as mixtures of choline chloride (99%) with ethylene glycol (ChCl-EG 1:2 mole ratio), malonic acid (ChCl-MA 1:1 mole ratio) and oxalic acid dihydrate (ChCl-OxA 1:1 mole ratio), respectively, all reagents being purchased from Aldrich. The appropriate binary mixtures were heated at above 90^{0}C for 30 min until homogeneous colourless ionic liquids are formed; then, the liquids were kept at room temperature. $BiCl_3$ or Bi_2O_3 (from Aldrich), and TeO_2 and SeO_2 (both from Alfa Aesar) were used as precursors for dissolved ionic species of bismuth, tellurium and selenium, respectively. The molarities were calculated using density values of 1.0963, 1.2065 and 1.2122 gcm^{-3} corresponding to ChCl-EG, ChCl-MA and ChCl-OxA mixtures, values determined in our laboratory at 60^{0}C working temperature.

Cyclic voltammograms and impedance (EIS) spectra were recorded using a Pt plate (0.5 cm^2) or a Cu disc (0.196 cm^2) as working electrodes in order to evidence the cathodic and anodic processes in non-stirred baths. Pt plate as auxiliary electrode and Ag wire (immersed in the same ionic liquid) as reference electrode were also used in the electrochemical cell. The stability in 0.5 M NaCl aqueous solution of films electrodeposited on commercial Cu sheets was determined by recording potentiodynamic polarization (Tafel) curves and EIS spectra. The corrosion cell contained Cu plate covered with BiTeSe film (0.636 cm^2 exposed area), a Pt plate as auxiliary electrode and Ag/AgCl as reference electrode.

Zahner IM 6 potentiostat and BioLogic Sci. Instr. potentiostat, both with FRA, were used for cyclic voltammetry (1-100 mVs^{-1} scan rate), potentiodynamic polarization (3 mVs^{-1} scan rate) and electrochemical impedance spectroscopy (10 mV *ac* voltage, 200 kHz - 50 mHz frequency range).

Results and discussions

Regarding the relatively good solubility of bismuth, tellurium and selenium precursor compounds in ChCl-EG, ChCl-MA or ChCl-OxA ionic liquids in such amounts to have a significant electrochemical response for Bi^{3+}, Te^{4+} and Se^{4+} ionic species, an assumption may be the presence of chloride anion Cl^- as ligand which forms complexes with these species; this complexation may improve the solubility of compounds and also the electrode potentials may close to each other in order to obtain a co-electrodeposition process. For instance, by dissolution of bismuth chloride (or bismuth oxide) precursor in the electrolyte we supposed the formation of $BiCl_4^-$ complex species, leading to a lower diffusive ionic species than simpler Bi^{3+} ion [16,17]. Correspondingly, the tellurite (TeO_2) or selenite (SeO_2) dissolved precursors should be converted into their chloride complexes; alternatively, they may be present as acids (H_2TeO_3, H_2SeO_3) due to a significant presence of water in the ionic liquid, especially in ChCl-OxA mixture.

Cyclic voltammograms

The analysis by cyclic voltammetry (CV) technique was carried out to determine the appropriate potential range in which Bi^{3+}, Te^{4+} and Se^{4+} cations co-deposit as BiTeSe films. We selected the CV curves obtained by sweeping the potential from stationary potential towards cathodic direction (up to -1.2 V limit) and returning to anodic region (up to limit of +1.2 V) and back. It is important to mention that the CVs on Pt in all background ionic liquids recorded in an enlarged potential range, -1.4V ÷ +1.4V, did not show any electrode process.

Comparative cyclic voltammograms of single Te^{4+} and Se^{4+} ionic species and of ternary mixture of Bi^{3+}, Te^{4+} and Se^{4+} ions recorded on Pt electrode in non-stirred choline chloride – ethylene glycol (1:2 mole ratio) ionic liquid are presented in figure 1.

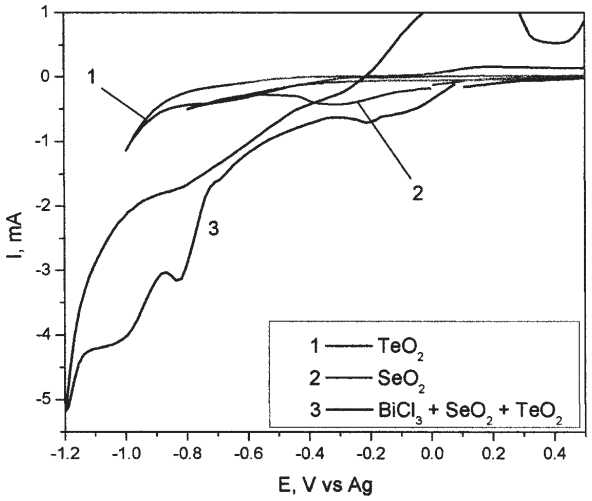

Fig. 1 Cyclic voltammograms on Pt electrode using ChCl-EG (1:2) ionic liquid containing: (1)5 mM TeO_2; (2) 10 mM SeO_2; (3) 4.8 mM $BiCl_3$ + 6.8mM TeO_2 +10 mM SeO_2. Scan rate v=50 mVs^{-1}, 60 ^{0}C

It is clearly noticed that, obeying the standard electrode potential scale [1], selenium element deposits at the most positive potentials (plateau of a current in the potential range -0.2 ÷ -0.4 V, curve 1) and deposition of tellurium element is at more negative potentials (plateau around -0.6 V, curve 2). As an interpretation of the cathodic branch of voltammogram for BiTeSe ternary film deposition (curve 3), three reduction processes can be identified, with three distinct potential ranges of limiting current or current peak. The first cathodic process that occurs on the curve 3 may be atributted to the Se^{4+} reduction, with the onset potential similar with curve 1 and a plateau in the potential range -0.1 ÷ -0.4 V). The second process may be attributed to co-deposition of ternary BiTeSe compound (with peak at -0.8 V). Finally, the third reduction process at potentials within -1.0 ÷ -1.2 V range may be due to deposition of a Bi-rich ternary BiTeSe layer. It results that Pt support first covers with a Se layer, and then the more cathodic polarization produces a co-deposition of Bi, Te and Se as ternary compound layer. An excessive cathodic polarization leads to a Bi massive deposition together with BiTeSe deposition and probably to the evolution of hydrogen or reduction of background electrolyte at over -1.2 V potential. Correspondingly, three distinguishable processes may be identified on the anodic branch of voltammogram: by scanning the potential towards positive values, the first two waves are attributed to anodic dissolutions of layers produced in the last reduction processes and the anodic peak (located at around +0.1 V) corresponds to the stripping of selenium layer previously formed on Pt.

Figure 2 compares the voltammetric response of the choline chloride – malonic acid (1:1 mole ratio) mixture in the presence of Bi^{3+} (as Bi_2O_3 in this system), Te^{4+} and Se^{4+} cations by varying the scan rate; the Pt electrode and working temperature were identical with binary system in figure 1. A narrow range of potentials and also low scan rates were selected for performing CVs in order to clearly show the existence of three couples of reduction/oxidation processes. All cathodic branches in this system have

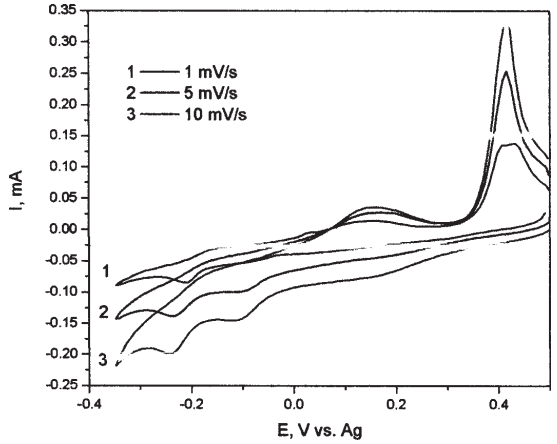

Fig. 2 Cyclic voltammograms on Pt electrode using ChCl-MA (1:1) ionic liquid containing 2.5 mM Bi_2O_3 + 2.5 mM TeO_2 +0.5 mM SeO_2 at various scan rates, 60 ^{0}C

relatively similar shape as in figure 1, with plateaux of current (first from +0.15 to 0 V, the second one from -0.1 to -0.18 V) or a peak current (located in the range -0.2 ÷ -0.25 V). We may suppose approximately a similar order of deposition: elemental Se layer, BiTeSe layer and Bi-rich BiTeSe layer. We observed that by increasing scan rate the last cathodic process is less evident, being overlapped with evolution of hydrogen (H^+ ion coming from malonic acid dissociation). All currents on voltammograms in this system have lower values than in ChCl-EG, an explanation being the lower concentration of Bi^{3+}, Te^{4+} and Se^{4+} ionic species. The difference in potential values comparing to figure 1 is certainly due to the shifting of potential for silver pseudoreference electrode by changing ionic liquid nature (malonic acid instead of ethylene glycol). On the anodic branches of voltammograms the first oxidation waves correspond to dissolution of Bi-rich ternary layer and BiTeSe layer, and the last anodic peak (in a sharp shape) represents a typical stripping process, which is consistent with the dissolution of electrodeposited selenium. On both branches of CVs in figure 2 all waves and peaks increase in height and remain at about the same potentials with various scan rates proving a diffusive control and relatively high reversibility of electrode processes.

Typical CVs recorded at various scan rates showing the electrochemical behaviour in conditions of simultaneous presence of Bi^{3+}, Te^{4+} and Se^{4+} ions in choline chloride - oxalic acid (1:1 mole ratio) mixture are presented in figures 3 (a,b). It can be seen that there are some differences comparing to the previous figures, although the sequence of electrode processes seems to be similar. As Figure 3a shows, at lower scan rates (3-20 mVs^{-1}) the Se deposition (represented by a plateau ranging from +0.4 to -0.1 V) is followed by a well defined peak (at -0.2 V) attributed to direct BiTeSe codeposition. However, the deposition of Bi in majority together with the ternary compound does not appear as distinct process because its wave is probably already overlapped with cathodic evolution of hydrogen (the continuous increase of current at over -0.25 V). This behavior may be explained by existence of significant concentration in H^+ ions, provided from both oxalic acid dissociation and water coming as dihydrate. Figure 3b presents supplementary two CV curves recorded at higher scan rates (50 and 100 mVs^{-1}). Now, the increase with scan rate of limiting current along the plateau of Se deposition is predominantly and, therefore, BiTeSe codeposition appears as a shoulder instead of a peak. Only

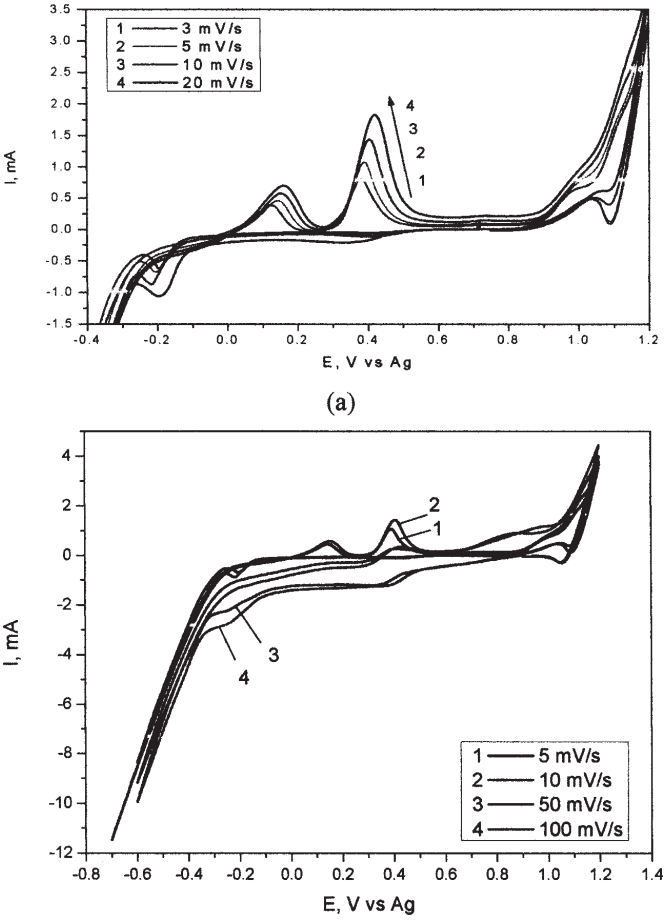

Fig. 3. Cyclic voltammograms on Pt for ChCl-OxA (1:1) ionic liquid containing 10 mM $BiCl_3$ +5 mM TeO_2 + 5 mM SeO_2 at various scan rates, 60 ^{0}C

two well contoured peaks are noticed on the anodic part of CVs, corresponding to consecutive dissolution of outer BiTeSe layer and of inner Se layer (as a sharp peak, typical for stripping). We notice that the other processes occurred in figures 3 to more positive potentials than +0.9 V are hardly to be explained, being certainly due to the content in oxalic acid and water of this ionic liquid system.

Interesting results were obtained during preliminary CV experiments in ChCl-OxA (1:1) ionic liquid by changing the nature of working electrode: Cu electrode was used instead of Pt working electrode. First it is worth to mention a displacement with *ca.* 600-700 mV more negatively of the stationary electrode potential. Figure 4 presents

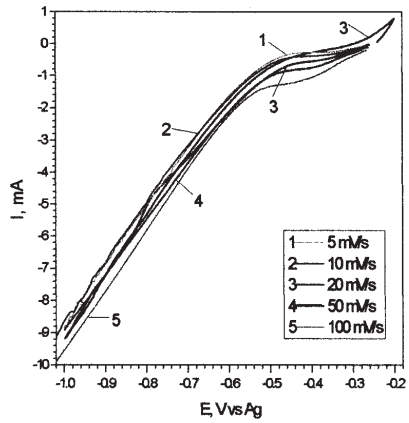

Fig. 4. Only cathodic branches (1,2,4,5) of CV curves and a full CV curve (3) on Cu electrode for ChCl-OxA (1:1) ionic liquid containing 10 mM $BiCl_3$ + 5 mM TeO_2 + 5 mM SeO_2; various scan rates, 60 ^{0}C

examples of cathodic branches of CV curves in ChCl-OxA ionic liquid on Cu electrode by keeping the same working conditions (temperature, scan rates) as in figures 3. It may be observed that the first process of Se deposition, that is located at most positive potential, is now almost hindered to be viewed; only it can be guessed this process as a small wave located around -0.27 V. So, we suppose that the main process of BiTeSe direct co-deposition occurs starting from -0.35 V and continues up to -0.5 V as a plateau (at low scan rates) or rather as a shoulder at higher scan rates. By polarizing more cathodically over -0.5 V, the continuous increase of current is responsible to the the third process discussed above (massive Bi deposition) that interfers with evolution of hydrogen. The anodic branches of CV curves show only a continuous increase of current, until around 0 V potential limit; we did not perform scanning at more positive potetials in order to prevent the electrochemical dissolution of copper support.

In a tentative to propose a mechanism of cathodic processes in two steps we may write the following equations:

$$Se^{4+} + 4\ e^- \rightarrow Se\ (film) \quad (1)$$

$$2\ Bi^{3+} + (3\text{-}y)\ Te^{4+} + y\ Se^{4+} + 18\ e^- \rightarrow Bi_2Te_{3-y}Se_y \quad (2)$$

In another way, we can take into consideration the equations proposed by all authors in aqueous solutions, where tellurium and selenium species were written as H_2TeO_3 and H_2SeO_3:

-for the first process (single deposition of Se with H^+ ions involvement):

$$H_2SeO_3 + 4\ e^- + 4\ H^+ \rightarrow Se + 3\ H_2O \quad (3)$$

-for the second process:

$$2\ Bi^{3+} + (3\text{-}y)\ H_2TeO_3 + y\ Se^{4+} + (12\text{-}4y)\ H^+ + 18\ e^- \rightarrow \rightarrow Bi_2Te_{3-y}Se_y + (9\text{-}3y)\ H_2O \quad (4)$$

Of course, the massive deposition of Bi means a direct reduction with three electrons of Bi^{3+} ion as a simple electrode process.

In general, in spite of the obvious differences in peak potential separation and peak shapes we can appreciate that all the reduction/oxidation processes are diffusion controlled and moderatelly irreversible, and this irreversibility degree may be due to a large non-compensated ohmic drop inside the ionic liquid.

Electrochemical impedance spectra

The cathodic formation of films was also studied by the electrochemical impedance spectroscopy (EIS) measurements at 60 ^{0}C. Figures 5 a,b show comparatively the recorded Nyquist and Bode (both impedance modulus and phase angle *vs.* frequency dependences) diagrams recorded on Pt in choline chloride – ethylene glycol ionic liquid. The electrode was polarized in the potential region where the reduction process has a significant cathodic current (peak or limiting current on CV curves). For tellurium deposition (curve 1) the Nyquist spectrum consists of a capacitive loop, followed by a straightline of unit slope. This shape clearly indicates a formation of Te film onto the Pt electrode surface. Curve 2 in the same figure represents two consecutive semicircles followed also by a straightline of unit slope and may be interpreted as a process where the first step is Se element deposition and the second step is a codeposition of TeSe semiconductor compound which has a composition of solid solution. Curve 3 corresponds to ternary codeposition resulting BiTeSe compound; the diameter of this semicircle (which represents the transfer charge resistance, R_{ct}) is now very small indicating a higher current of the faradaic process. It can be seen from figure 5b that according to the phase angle values, TeSe semiconductor has the highest insulating properties (-60^0 phase angle) due to its high content of selenium, Te film is also a good semiconductor material (-55^0), but the obtained BiTeSe film has already a metallic character (-30^0 phase angle), explained by a significant content of Bi and low content in Se in the ternary compound.

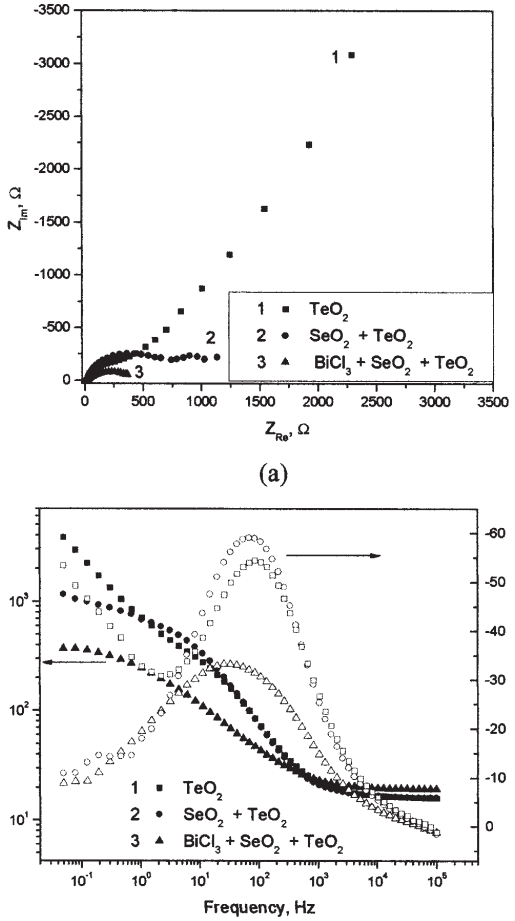

Fig. 5. Comparison between Nyquist (a) and Bode (b) spectra recorded at 60 ^{0}C on Pt in ChCl-EG (1:2 mole ratio) containing 5 mM TeO_2 (curve 1, -0.3 V potential); 2.5 mM TeO_2 + 10 mM SeO_2 (curve 2, -0.6 V potential); 4.8 mM $BiCl_3$ +6.8 mM TeO_2+10 mM SeO_2 (curve 3, -0.8 V potential). Stationary potential of Pt: +0.1V vs. Ag reference

The impedance behaviour of Pt and Cu electrodes during codeposition of bismuth, tellurium and selenium in choline chloride – oxalic acid ionic liquid is also revealed by recording EIS spectra as Nyquist and Bode (only phase angle vs. frequency) diagrams. We have obtained impedance data by polarizing the electrode at different electrode potentials, *ie* in the potential region of low cathodic polarization (where Se deposition is predominantly), then within the potential ranges with peak or limiting current for Bi, Te and Se codeposition, and finally in the area of very negative values, where the massive deposition may interfer with hydrogen evolution or reduction of blank electrolyte. Figures 6,7 present the EIS spectra obtained on Pt electrode according to this strategy. For the first process, which was assigned to deposition of selenium element, the Nyquist spectra in figure 6 are represented as a capacitive semicircle at high frequencies followed by a straightline of unit slope.

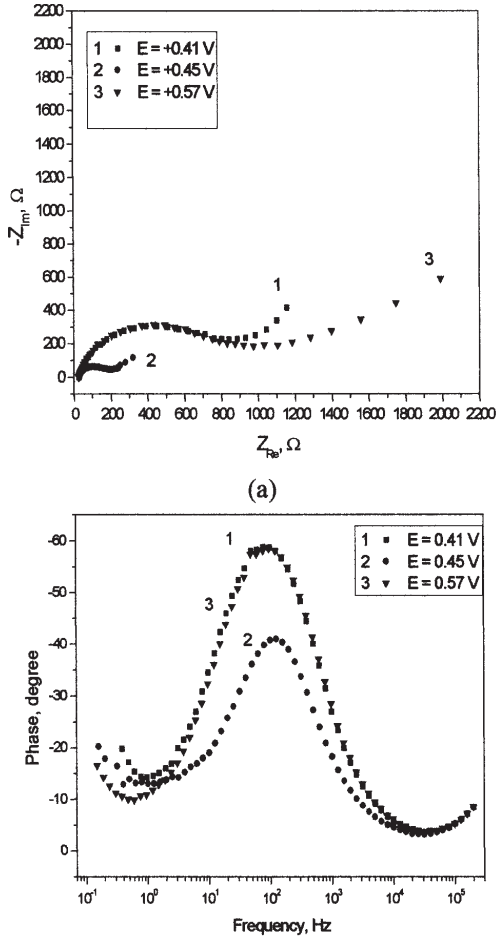

Fig. 6. Nyquist (a) and Bode (b) spectra recorded at 60 ^{0}C on Pt in ChCl-OxA (1:1 mole ratio) containing 10 mM $BiCl_3$ + 5 mM TeO_2 + 5 mM SeO_2 at the potential region of low cathodic polarization (onset of deposition of Se). Stationary potential of Pt: +0.64 V vs. Ag reference

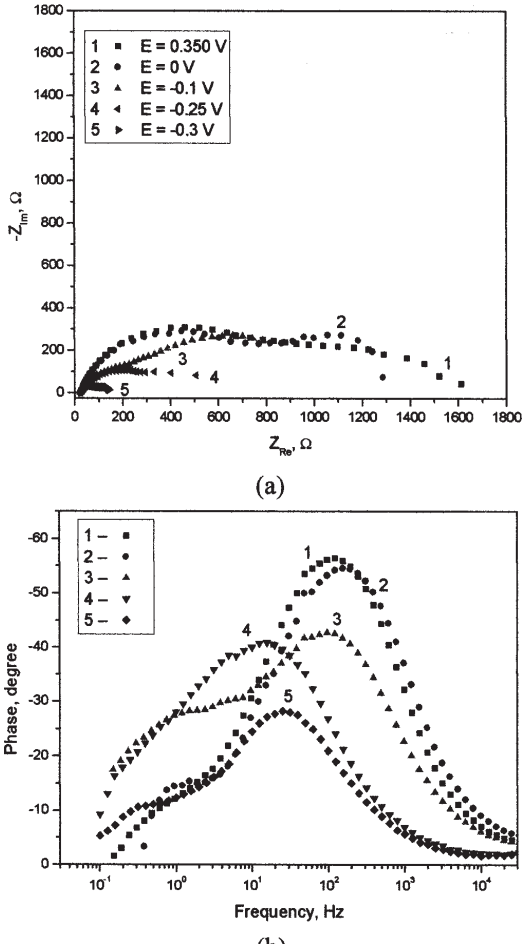

Fig. 7. Nyquist (a) and Bode ((b), only phase angle) spectra recorded at 60 ^{0}C on Pt in the same system ChCl-OxA (1:1 mole ratio) containing 10 mM $BiCl_3$ + 5mM TeO_2 + 5 mM SeO_2; the potential region of high cathodic polarization (deposition of Se and BiTeSe ternary compound at more negative values). Stationary potential of Pt: +0.64 V vs. Ag reference. Curves: (1) +0.35V; (2) 0V; (3) -0.10V; (4) -0.20V; (5) -0.30V

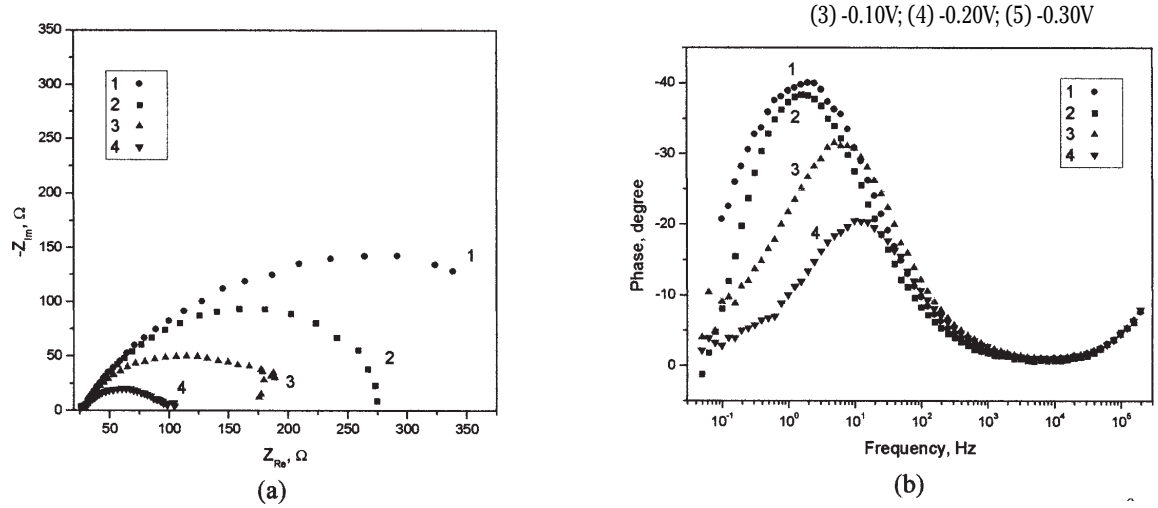

Fig. 8. Nyquist (a) and Bode (b) spectra recorded at 60 ^{0}C on Cu in the same system ChCl-OxA (1:1 mole ratio) containing 10 mM $BiCl_3$ + 5mM TeO_2 + 5 mM SeO_2; different cathodic potentials. Stationary potential of Cu: -0.26 V vs. Ag reference. Curves: (1) -0.35V; (2) -0.40V; (3) -0.45V; (4) -0.50V

By gradually polarizing Pt electrode in negative direction, first successive Nyquist and Bode diagrams (fig. 7 a,b) suggest the existence of two consecutive deposition processes, as two semicircles or two phase angle maxima in the potential region where deposition of both Se and BiTeSe takes place. For more negative potentials than -0.25 V, the deposition of ternary BiTeSe film on already deposited selenium becomes predominantly, so a single Nyquist semicircle and a single phase angle maximum is recorded. Normally, the magnitude of semicircle diameters are different, because the diameter decreases with cathodic polarization indicating an increase of charge transfer rate and faradaic current during deposition. All Nyquist diagrams do not show perfect semicircles, rather depressed semicircles, and this fact has been attributed to frequency dispersion due to inhomogeneity and roughness of electrode surface.

The EIS diagrams obtained for Cu electrode (fig. 8) confirm the interpretation of cyclic voltammetry curves recorded using this electrode, respectively a quite direct BiTeSe deposition followed by massive deposition of Bi at very negative potentials. Thus, the successive Nyquist single semicircles (fig. 8a) decrease gradually in their diameter with cathodic polarization and the successive Bode curves (fig. 8b) decrease dramatically their values of phase angle maxima, reaching even to -20^0 for -0.50 V polarization, that is a phase angle value characteristic for a metallic film.

We can validate and quantitatively interpret the experimental impedances obtained, by modeling the electrode process using an equivalent electrical circuit. Figure 9 shows an equivalent circuit established using the specialized software Zview 2.90c (Scribner Assoc.) and employed to fit the EIS experimental data. Regarding this circuit, the whole impedance of the electrode is represented as a series connection of the solution resistance Rs and a parallel circuit of the double-layer capacitance (which is generally denoted as Cdl) and charge transfer resistance, Rct, here denoted as R1. However, we showed that the electrode surface is modified by microscopic roughness caused by scratches, pits, etc., and also its capacitance is dispersed, being influenced by slow adsorption of ions and chemical inhomogeneities of the surface. In such cases a constant phase element CPE is often introduced instead of Cdl. Its impedance is given by:

$$Z_{CPE} = \frac{1}{T(j\omega)^P} \quad (5)$$

where T is a constant in F cm^{-2} s^{P-1}, $j=\sqrt{-1}$, ω is angular frequency ($\omega = 2\pi f$, f - *ac* frequency, Hz) and P is an exponent. Only when P =1, T≡ C_{dl} and purely capacitive behavior is obtained. In general, eq. (5) may represent pure capacitance for P = 1, infinite Warburg impedance for P = 0.5, pure ohmic resistance for P = 0 and pure inductance for P = -1. W1 is a Warburg element of linear finite-length diffusion.

Table 1 contains the values of equivalent circuit elements for the best fitting of experimental data representing BiTeSe deposition in choline chloride + oxalic acid (1:1) ionic liquid, 60 ^{0}C. It may be seen that the changes in EIS spectra after polarization of Pt or Cu electrode at different cathodic overpotentials were well reflected in the fitted parameters.

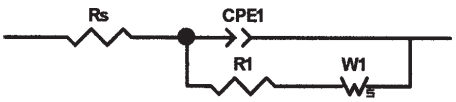

Fig. 9 Scheme of equivalent electrical circuit for BiTeSe films obtained from choline chloride + oxalic acid (1:1) ionic liquid, 60 ^{0}C. Circuit components: Rs – solution ohmic resistance; CPE 1 – constant phase element replacing double layer capacitance; R1– charge transfer resistance (R_{ct} -for cathodic deposition) or polarization resistance (R_P -for corrosion tests); W - Warburg diffusion impedance

The solution resistance Rs is related to electrical conductivity of electrolyte which has a relatively lower value for ionic liquid than for aqueous solution. Differences in Rs shown in tables 1 and 2 are due to different positions of the electrodes in electrochemical cell. The evolution of charge transfer resistance Rct corresponds to evolution of faradaic current in the cyclic voltammograms at gradual cathodic polarization. All double layer pseudo-capacitances (expressed as CPE1-T) are almost similar for both electrodes and all potentials, exception being values for massive deposition (Bi and BiTeSe) which are of one order of magnitude higher. The exponent CPE1-P has values in a narrow region of 0.7-0.86, exhibiting a similar deviation of the interface from a pure capacitor.

Preparation and corrosion behaviour of BiTeSe films deposited on Cu support

BiTeSe film samples were prepared under potentiostatic or galvanstatic control on copper sheets from mixtures of choline chloride with malonic acid or with oxalic acid at 60 ^{0}C, without stirring the ionic liquid bath. Table 3 presents the operating conditions in both ionic liquid electrolytes and some characteristics of BiTeSe deposits (aspect, adherence on copper support).

We consider that deposits formed in shorter time (BiTeSe-1 and BiTeSe-3 samples) have a composition with relatively higher Se content than the other deposits. We noticed that the BiTeSe films electrodeposited in conditions of long-time electrolysis (60 or 120 min) possess a smoother surface and more compact structure than those prepared by the short-time electrolysis. It is also confirmed (from color changes) that electrodeposition at more negative potentials leads to an increase of bismuth content in the BiTeSe film. So, it is clear that the characteristics of

Table 1

VALUES OF COMPONENTS IN THE EQUIVALENT CIRCUIT USED FOR BEST FITTING OF EIS DATA FOR BiTeSe DEPOSITION ON Pt ELECTRODE. IONIC LIQUID: ChCl-OxA (1:1) + 10 mM $BiCl_3$ + 5 mM TeO_2 + 5 mM SeO_2, 60 ^{0}C

Component in scheme of Fig. 9	Values of circuit components for various cathodic potentials							
	+0.57 V	+0.45 V	+0.41 V	+0.35 V	0 V	-0.10 V	-0.20 V	-0.30 V
R_s, Ω	23.6	23.0	24.2	23.8	23.2	24.0	22.5	25.2
CPE1-T ×10^6 (pseudo-capacitance), F s^{P-1}	71	33	28	28	27	82	421	459
CPE1-P exponent	0.83	0.86	0.87	0.84	0.82	0.77	0.69	0.76
R_1 (R_{ct}), Ω	156	783	821	819	832	197	410	82
W1-R, Ω	263	274	840	537	328	841	2793	52
W1-T (pseudo-inductance), H s^{P-1}	3.54	0.36	1.19	0.51	0.23	1.67	4.42	1.70
W1-P exponent	0.48	0.58	0.55	0.53	0.65	0.37	0.78	0.35

Component in scheme of Fig. 9	Values of components in the equivalent circuit for various cathodic potentials				
	-0.35V	-0.40V	-0.45V	-0.50 V	-0.60 V
R_s, Ω	22.7	21.4	23.6	23.0	30.9
CPE1-T $\times 10^6$ (pseudocapacitance), F s^{P-1}	50	94	71	33	743
CPE1-P exponent	0.86	0.79	0.83	0.86	0.80
R_1 (R_{ct}), Ω	779	147	156	783	31
W1-R, Ω	1958	90	263	274	5
W1-T (pseudoinductance), H s^{P-1}	1.06	0.06	3.54	0.36	0.25
W1-P exponent	0.31	0.44	0.48	0.58	0.42

Table 2
VALUES OF COMPONENTS IN THE EQUIVALENT CIRCUIT USED FOR BEST FITTING OF EIS DATA FOR BiTeSe DEPOSITION AT VARIOUS CATHODIC POTENTIALS ON Cu ELECTRODE. IONIC LIQUID: ChCl-OxA (1:1) + 10 mM $BiCl_3$ + 5 mM TeO_2 + 5 mM SeO_2, 60 °C

Bath	Sample	Controlled current or potential	Electrolysis time, min	Characteristics of deposit
ChCl-MA (1:1) +2.5 mM Bi^{3+} + 2.5 mM Te^{4+} + 0.5 mM Se^{4+}	BiTeSe-1	-0.55 V vs. Ag ref.	5	Uniform, light grey, adherent
	BiTeSe-2	-0.55 V vs. Ag ref.	10	Uniform, grey, adherent
	BiTeSe-3	2.5 mA/cm^2	10	Uniform, grey-black, adherent
	BiTeSe-4	3 mA/cm^2	60	Uniform, compact bright grey-black, adherent
ChCl-Ox.A (1:1) +10 mM Bi^{3+} + 5 mM Te^{4+} + 5 mM Se^{4+}	BiTeSe-I	-0.35 V vs. Ag ref.	120	Uniform, bright black, adherent
	BiTeSe-II	-0.42 V vs. Ag ref.	60	Uniform, compact, bright black, adherent

Table 3
OPERATION CONDITIONS DURING PREPARATION OF BiTeSe SAMPLES ON COPPER SHEET USING ChCl-MA AND ChCl-OxA IONIC LIQUIDS, 60 °C

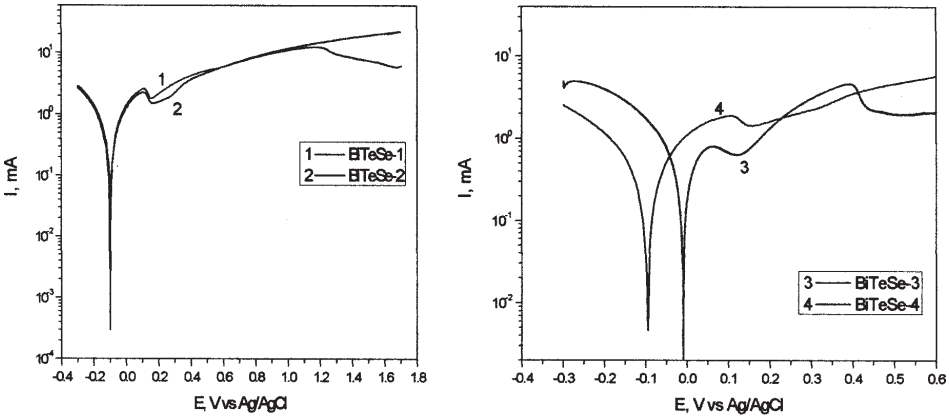

(a) (b)

Fig. 10. Semilogarithmic potentiodynamic polarization plots for BiTeSe samples 1,2,3,4 (table 3) in 0.5 M NaCl aqueous solution; 3 mVs^{-1} scan rate, 25 °C, 0.636 cm^2 exposed area

deposits may be easily controlled by selecting the appropriate electrolysis conditions.

Samples elaborated under potentiostatic (denoted as 1,2) or galvanostatic (denoted as 3,4) control using bath containing choline chloride - malonic acid (1:1) mixture +2.5 mM Bi^{3+} + 2.5 mM Te^{4+} + 0.5 mM Se^{4+} were tested for their corrosion resistance. Figures 10 a,b show the potentiodynamic polarization curves recorded for these samples. Also, a comparison of electrochemical impedance spectra (EIS) recorded by polarizing BiTeSe films at different anodic overpotentials can be seen in figures 11-14. We mention that more corrosion data regarding our investigations in various liquid media (including ionic liquids) were reported in another paper [18].

In all cases presented in figures 10 the Tafel polarization curves were plotted starting from the stationary potential firstly toward cathodic direction and then toward anodic direction. The increase in current in the first part of anodic branch starting from stationary potential is indicative of the active dissolution of BiTeSe film. However, at a potential around +0.1 V *vs.*Ag/AgCl reference electrode a decrease in the current for all samples may suggests a passivation process that may be due to the insoluble corrosion products formed and adsorbed temporary on the surface. Then, in more positive part of Tafel curve the film returns to an active state and continues to be corroded with a quite moderate constant rate; only samples with more Se content (BiTeSe-1 and BiTeSe-3) show a new passivation process at high anodic polarization. We consider that the cathodic process when the applied potential increased into the negative region (cathodic branch of Tafel curves) corresponds mainly to the evolution of the hydrogen that is an activation-controlled process.

Estimation of the corrosion parameters was made using the corrosion soft of potentiostats, the characteristic corrosion data being listed in table 4. It seems, from corrosion currents values, that more corrosion resistance is reached by galvanostatic electrolysis; (samples 3 and 4); also, in these cases the cathodic (*bc*) and anodic (*ba*) Tafel slopes were obtained in a narrow range (83-94 mV/decade).

Also, a comparison of electrochemical impedance spectra (EIS data) recorded by polarizing BiTeSe films in 0.5 M NaCl solution at different anodic overpotentials exhibited a quite similar corrosion behaviour (figs. 11-14).

BiTeSe film	Values of parameters			
	i_{corr}, mA	E_{corr}, V *vs.* Ag/AgCl	Tafel slopes, mV/dec	
			b_a	b_c
BiTeSe-1	0.50	-0.100	245	202
BiTeSe-2	0.38	-0.098	200	180
BiTeSe-3	0.21	-0.020	90	83
BiTeSe-4	0.16	-0.093	94	92

Table 4
CORROSION DATA ESTIMATED FROM TAFEL POLARIZATION CURVES OF BiTeSe FILMS (BiTeSe 1,2,3,4; 0.636 cm^2 EXPOSED AREA), IMMERSED IN 0.5 M NaCl AQUEOUS SOLUTION AT 25 ^{0}C

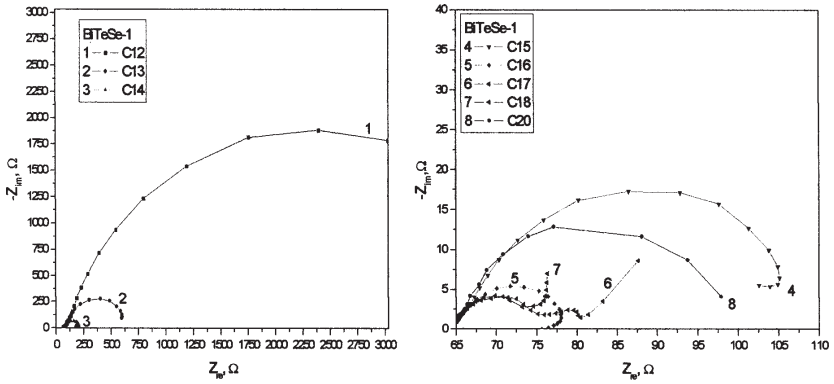

Fig. 11. EIS Nyquist plots for BiTeSe-1 sample at various anodic polarization potentials in 0.5 M NaCl aqueous solution; 25 ^{0}C, 0.636 cm^2 exposed area

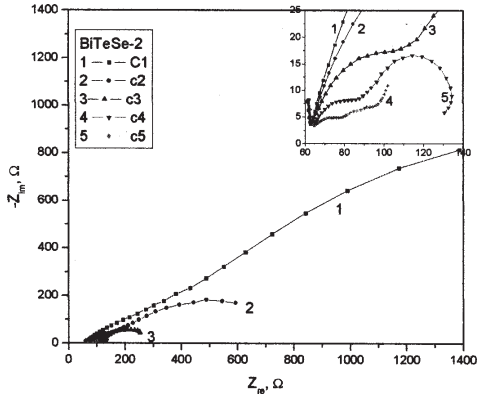

Fig. 12. EIS Nyquist plots for BiTeSe-2 sample at various anodic polarization potentials in 0.5 M NaCl aqueous solution; 25 ^{0}C, 0.636 cm^2 exposed area

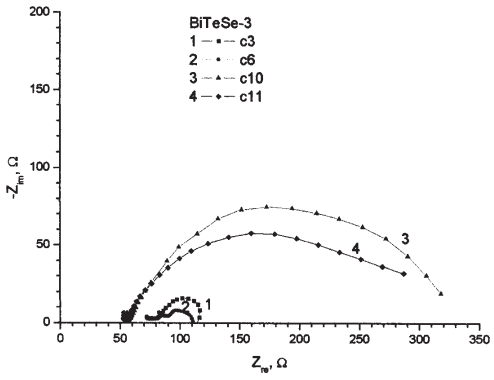

Fig. 13. EIS Nyquist plots for BiTeSe-3 sample at various anodic polarization potentials in 0.5 M NaCl aqueous solution; 25 ^{0}C, 0.636 cm^2 exposed area

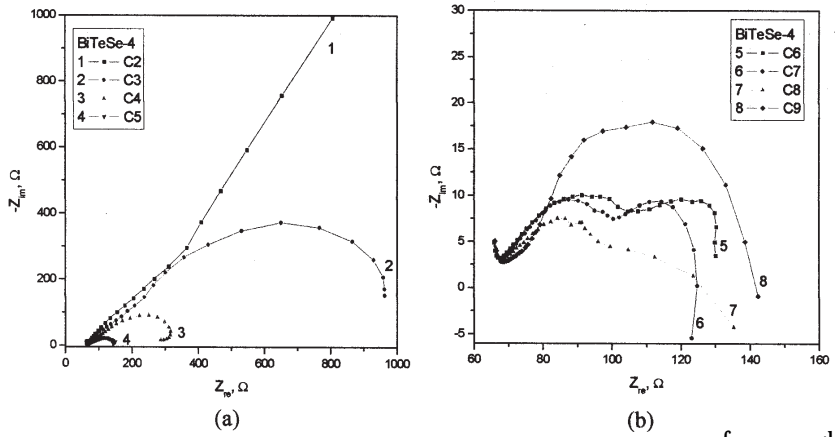

Fig. 14. EIS Nyquist plots for BiTeSe-4 sample at various anodic polarization potentials in 0.5 M NaCl aqueous solution; 25 ^{0}C, 0.636 cm^2 exposed area

Nyquist plots are generally in a shape of capacitive arc; the diameter of semicircles is gradually decreased by polarizing anodically, proving decreased polarization resistance, Rp, *i.e.* an increase of corrosion current, as expected. However, the shape of impedance spectra is not ideal semicircle. We consider that the factors such as surface roughness, the existence of corrosion products or formation of passive films can contribute to a deviation in ideal semicircle

The behaviour of deposit corrosion was simulated with some equivalent electric circuits as models; one was shown in figure 9 and the other two models are presented in figures 15. The circuit in figure 15a is a simple Randles

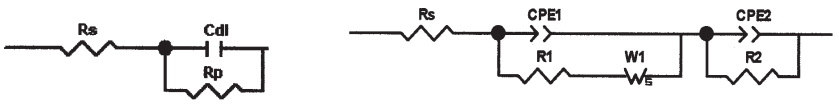

Fig. 15. Two new equivalent electrical circuits proposed as models for fitting the EIS data in corrosion tests

Component in scheme of Fig. 9	Values of components in the equivalent circuit for various anodic polarization							
	-0.10 V	-0.08 V	-0.06 V	-0.03 V	0 V	+0.05 V	+0.10 V	+0.15 V
R_s, Ω	64.0	66.4	65.9	64.4	59.6	63.4	63.7	64.4
CPE1-T $\times 10^6$ (pseudocapacitance), F s^{P-1}	396	536	438	745	2730	662	156	2370
CPE1-P exponent	0.71	0.74	0.83	0.75	0.17	0.69	0.82	0.79
R_1 (R_P), Ω	4500	575	130	45	14	10	9	29
W1-R, Ω	5414	705	150	43	16	11	10	122
W1-T (pseudoinductance), H s^{P-1}	1.04	0.23	0.09	0.03	0.02	0.01	0.01	4.12
W1-P exponent	0.74	0.61	0.53	0.51	0.46	0.46	0.45	0.97

Table 5
FITTING PARAMETERS FOR BiTeSe-1 SAMPLE ANODICALLY POLARIZED IN 0.5 M NaCl AQUEOUS SOLUTION USING EIS TECHNIQUE, 25 °C. EXPOSED SURFACE: 0.636 cm^2

Component in scheme of Fig. 9	Values of components in the equivalent circuit for various anodic polarization				
	-0.10 V	-0.08 V	-0.06 V	-0.03 V	0 V
R_s, Ω	60.5	60.6	62.5	61.3	49.2
CPE1-T $\times 10^6$ (pseudocapacitance), F s^{P-1}	237	213	55	190	6932
CPE1-P exponent	0.59	0.60	0.75	0.62	0.18
R_1 (R_P), Ω	2650	970	79	32	82
W1-R, Ω	2444	586	214	60	65
W1-T (pseudoinductance), H s^{P-1}	9.37	3.80	2.31	0.42	13.12
W1-P exponent	0.42	0.39	0.33	0.35	0.81

Table 6
FITTING PARAMETERS FOR BiTeSe-2 SAMPLE ANODICALLY POLARIZED IN 0.5 M NaCl AQUEOUS SOLUTION USING EIS TECHNIQUE, 25 °C. EXPOSED SURFACE: 0.636 cm^2

Component in scheme of Fig. 15a	Values of components in the equivalent circuit (15a) for various anodic potentials			
	0 V	+0.10 V	+0.15 V	+0.25 V
R_s, Ω	81	83	81	87
$C_{dl} \times 10^6$, F	1020	1210	2500	838
R_1 (R_P), Ω	40	24	272	221

Table 7
FITTING PARAMETERS FOR BiTeSe-3 SAMPLE ANODICALLY POLARIZED IN 0.5 M NaCl AQUEOUS SOLUTION USING EIS TECHNIQUE, 25 °C. EXPOSED SURFACE: 0.636 cm^2

Component in scheme of Fig. 9	Values of components in the equivalent circuit (15b) for various anodic potentials							
	-0.18 V	-0.13 V	-0.08 V	-0.03 V	+0.02 V	+0.07 V	+0.12 V	+0.17 V
R_s, Ω	63.9	63.9	64.0	63.8	62.8	64.2	64.6	65.8
CPE1-T $\times 10^6$ (pseudocapacitance), F s^{P-1}	206	232	248	467	2490	1835	1982	41
CPE1-P exponent	0.96	0.62	0.61	0.54	0.38	0.43	0.43	0.79
R_1 (R_P), Ω	1044	873	277	89	68*	50*	41*	78
W1-R, Ω	6430	888	245	59	9.6	12	10	64
W1-T (pseudoinductance), H s^{P-1}	4.021	0.40	0.13	0.03	0.52	0.55	0.13	0.15
W1-P exponent	0.41	0.49	0.43	0.40	0.53	0.61	0.70	0.44

*Values of diameters for the first semicircle (scheme Fig. 15b)

Table 8
FITTING PARAMETERS FOR BiTeSe-4 SAMPLE ANODICALLY POLARIZED IN 0.5 M NaCl AQUEOUS SOLUTION USING EIS TECHNIQUE, 25 °C. EXPOSED SURFACE: 0.636 cm^2

circuit with a pure capacitor having a double-layer capacitance (Cdl). The second one model (fig. 15b) contains a scheme where the connection of the polarization resistance (denoted as R_1) and W1 in parallel with a constant phase element (CPE1) is in series with a second parallel connection of BiTeSe film components: ohmic resistance (R_2) and its capacitance (CPE2).

Tables 5-8 contains the fitting data using circuit models from Figures 9 and 15a. Although we did not perform calculations with with circuit model from figure 15b, we consider that this last scheme is better suitable for interpretation of several EIS spectra showing two time constants (two semicircles or two phase angle maxima). The obtained data demonstrate clearly that BiTeSe films formed by long-time electrolysis (BiTeSe-2 and BiTeSe-4) have a higher corrosion resistance (they have higher Rp values) than films formed in short time. The highest metallic character seems to be for BiTeSe-4 proving that it has a composition with higher Bi content.

Conclusions

The present electrochemical investigation showed that BiTeSe films can be successfully deposited from all three ionic liquids electrolytes consisting in binary mixtures of choline chloride with ethylene glycol, malonic acid and oxalic acid, respectively. From cyclic voltammetry and impedance experiments carried out at 60 °C using Pt and

Cu electrodes there were evidenced the characteristics of cathodic processes and, especially, it was possible to predict the potential ranges for codeposition of Bi, Te and Se as ternary BiTeSe compound.

The electrodeposition of BiTeSe films takes place from all electrolytes on a Se-covered substrate. Also, these films were formed at less negative potentials than for deposition of singular Se (or Te films). In general, the corrosion resistance of BiTeSe films in 0.5 M NaCl solution was similar with other semiconductor films containing Se or Te and in the evolution of corrosion may possible occur retaining of corrosion products and formation of a passive film.

Finally, we mention that the preparation of BiTeSe films by electrodeposition technique from choline chloride – oxalic acid ionic liquid was reported for the first time in literature.

Acknowledgements: One of the authors recognises support from the European Social Fund through POSDRU/88/1.5/S/60203 Project.

References

1. BOUROUSHIAN, M., Electrochemistry of Metal Chalcogenides, Springer-Verlag, Berlin, 2010, p. 60
2. XIAO, F., HANGARTER, C., YOO, B., RHEEM, Y., LEE, K.H., MYUNG, N.V., Electrochim. Acta **53**, 2008, p. 8103
3. BOULANGER, C., J. ELECTRON. MATER., **39** (9), 2010, p. 1818
4. MARTIN-GONZALEZ, M., SNYDER, G.J., PRIETO, A.L., GRONSKY, R., SANDS, T., STACY, A.M., Nano Lett., **3** (7), 2003, p. 973
5. MICHEL, S., STEIN, N., SCHNEIDER, M., BOULANGER, C., LECUIRE, J.M., J. Appl. Electrochem., **33**, 2003, p. 23.
6. ZIMMER, A., STEIN, N., TERRYN H., BOULANGER, C., J. Phys. Chem. Solids, **68,** 2007, p. 1902
7. 1. MICHEL, S., DILIBERTO, S., STEIN, N., BOLLE, B., BOULANGER, C., J. Solid State Electrochem., **12**, 2008, p. 95
8. BU, L.X., WANG, W., WANG, H., Appl. Surf. Sci., **253** (6), 2007, p. 3360; Mater. Res. Bull., **43**, 2008, p. 1808
9. LI, S.H., SOLIMAN, H.M.A., ZHOU, J., TOPRAK, M.S., MUHAMMED, M., PLATZEK, D., ZIOLKOWSKI, P., MULLER, E., Chem. Mater., **20**, 2008, p. 4403
10. ZHOU, J., LI, S., SOLIMAN, H.M.A., TOPRAK, M.S., MUHAMMED, M., PLATZEK, D., MULLER, E., J. Alloys Compd., **471**, 2009, p. 278
11. KÖSE, H., BIÇER, M., TÜTÜNO LU, C., AYDIN, A.O., ŢIŢMAN, I., Electrochim. Acta, **54**, 2009, p. 1680
12. ZEIN EL ABEDIN, S., ENDRES, F., chapter 7 in: Molten salts and ionic liquids. Never the twain?, M. Gaune-Escard, K.R. Seddon, Editors, J. Wiley & Sons, New York, 2010, p. 85
13. ABDEL AAL, A.A., VOIGTS, F., CHAKAROV, D., ENDRES, F., Electrochim. Acta, **56** (28), 2011, p. 10295
14. STEICHEN, M., DALE, P., Electrochem. Commun., **13** (8), 2011, p. 865
15. GOLGOVICI, F., COJOCARU, A., NEDELCU, M., VISAN, T., Chalcog. Lett., **6** (8), 2009, p. 323
16. GOLGOVICI, F., COJOCARU, A., NEDELCU, M., VISAN, T., J. Electron. Mater., **39,** 2010, p. 2079
17. GOLGOVICI, F., COJOCARU, A., ANICAI, L., VISAN, T., Mater. Chem. Phys., **126**, 2011, p. 700
18. AGAPESCU, C., GOLGOVICI, F., COJOCARU, A., COTARTA, A., UPB Sci. Bull. B., **74** (2), 2012, p. 25
19. COJOCARU, A., SIMA, M., Rev. Chim. (Bucharest), **63**, no. 2, 2012, p. 217
20. ABBOTT, A.P., CAPPER, G., DAVIES, D., MUNRO, H., RASHEED, R.K., TAMBYRAJAH, V., Chem. Commun., 2001, p. 2010
21. BHATTACHARYA, C., DATTA, J., Mater. Chem. Phys., **89**, 2005, p. 170

Manuscript received: 14.06.2012